RESEARCH ARTICLE | APRIL 05 2010

Biphase micro/nanometer sized single crystals of organic semiconductors: Control synthesis and their strong phase dependent optoelectronic properties

Chengliang Wang; Yaling Liu; Zhongming Wei; Hongxiang Li; Wei Xu; Wenping Hu

Appl. Phys. Lett. 96, 143302 (2010)
https://doi.org/10.1063/1.3383222

Biphase micro/nanometer sized single crystals of organic semiconductors: Control synthesis and their strong phase dependent optoelectronic properties

Chengliang Wang,[1,2] Yaling Liu,[3] Zhongming Wei,[1,2] Hongxiang Li,[4,a)] Wei Xu,[1] and Wenping Hu[1,a)]
[1]*Beijing National Laboratory for Molecular Sciences, Key Laboratory of Organic Solids, Institute of Chemistry, Chinese Academy of Sciences, Beijing 100190, People's Republic of China*
[2]*Graduate University of the Chinese Academy of Sciences, Beijing 100039, People's Republic of China*
[3]*National Center for Nanoscience and Technology, Beijing 100190, People's Republic of China*
[4]*Shanghai Institute of Organic Chemistry, Chinese Academy of Sciences, Shanghai 200032, People's Republic of China*

(Received 10 October 2009; accepted 8 March 2010; published online 5 April 2010)

The control synthesis of α and β phase micro/nanometer sized single crystals of semiconductor 9,10-bis(phenylethynyl)anthracene were achieved; the device performance of individual α and β phase single crystals showed strong phase dependence; devices of β phase single crystals exhibited very high photoswitch performance (on/off current ratio $\sim 6\times 10^3$, one of the highest values reported for organic materials), and those of α phase displayed high field-effect performance. © *2010 American Institute of Physics*. [doi:10.1063/1.3383222]

Organic single crystal devices combined the merits of single crystals (perfect molecular ordering and free of grain boundaries),[1,2] and the advantages of organic semiconductors (facile modification, tunable property, flexibility, low-cost, and lightweight).[3,4] They can reveal the intrinsic properties of materials, and be helpful to understand the structure-property relationships (including the influence of chemical structures, molecular interactions and molecular packing on the properties) of organic semiconductors and the working mechanism of devices.

Photoswitches are devices that use light to control the currents between electrodes. They have been found wide applications in photodetectors, sensors, photoswitch circuits, logic circuits, and so on.[5–11] Similar to field-effect transistors (FETs) which are "three-terminal" devices with source, drain, and gate electrodes, photoswitches can also be seen as "three-terminal" devices with light as unconventional gate.[5,6] Till now, some photoswitches based on inorganic materials with light/dark current ratio up to 10^3 have been reported.[7,8] However, there are few reports about photoswitches based on organic materials though they are superior to their inorganic counterparts in some aspects as mentioned above, and the reported performance of organic photoswitches are extremely lower than that of inorganic materials (the light/dark current ratio of organic photoswitches are usually about 10^2).[9–11] Herein, using 9,10-bis(phenylethynyl)anthracene (**BPEA**) as candidate, we demonstrated a high performance single crystal photoswitch with light/dark current ratio up to 6×10^3, one of the highest values reported for organic semiconductors.

BPEA is well known for its strong fluorescent property and high emission efficiency and has been broadly used in fluorescent dyes and organic light emission diodes etc.[12–14] Single crystals of **BPEA** have two phases (Fig. 1). In one phase (we named it as phase α),[15] **BPEA** has nearly planar conformation in crystals [Figs. 1(c) and 1(e)], and the crystals belong to a crystal system of monoclinic space group C_2/c with unit-cell parameters of $a=22.866(5)$, $b=5.3567(11)$, $c=16.930(3)$ Å, and $\beta=99.72(3)°$. In the other phase (we named it as phase β),[13,14] **BPEA** displays nonplanar structure in the crystals [Figs. 1(d) and 1(f)]. In this phase, the crystals belong to orthorhombic space group *Pbcn* with unit-cell parameters of $a=24.305(4)$, $b=11.512(1)$, $c=7.099(1)$ Å, and $\alpha=\beta=\gamma=90°$. Though both phases adopt herringbone packing, their herringbone angles showed big difference. For phase α, the herringbone angle is about 79.2° [Fig. 1(a)], while for phase β the herringbone angle is about 27.3° [Fig. 1(b)]. This means that compared with phase α, the molecular arrangement in phase β is more close to face-to-face packing (or lamellar stacking). These differences made **BPEA** a good candidate to study the relationship between structures and properties (or phase dependent properties). In this communication, the control synthesis of micro/nanosized single crystals of α and β phase **BPEA** was achieved. The strong phase dependent optoelectronic properties of these single crystals were also studied.

We have reported that by drop casting a chlorobenzene

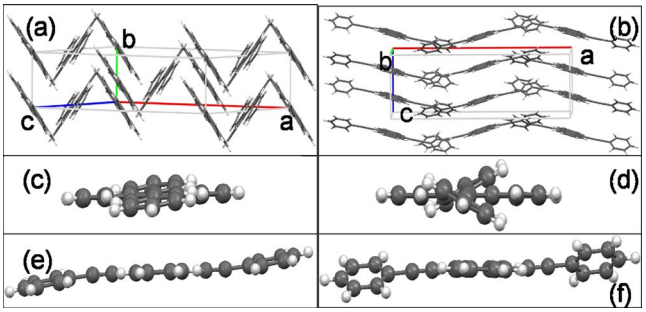

FIG. 1. (Color online) The single crystal diffraction results of α and β phase BPEA. (a) and (b) Packing diagram, (c) and (d) molecular structure viewed along the long axis, and (e) and (f) molecular structure viewed along the short axis. (a), (c), and (e) phase α; (b), (d), and (f) phase β.

a)Authors to whom correspondence should be addressed. Electronic addresses: lhx@mail.sioc.ac.cn and huwp@iccas.ac.cn. FAX: 86-21-54925024. Tel.: 86-21-54925024.

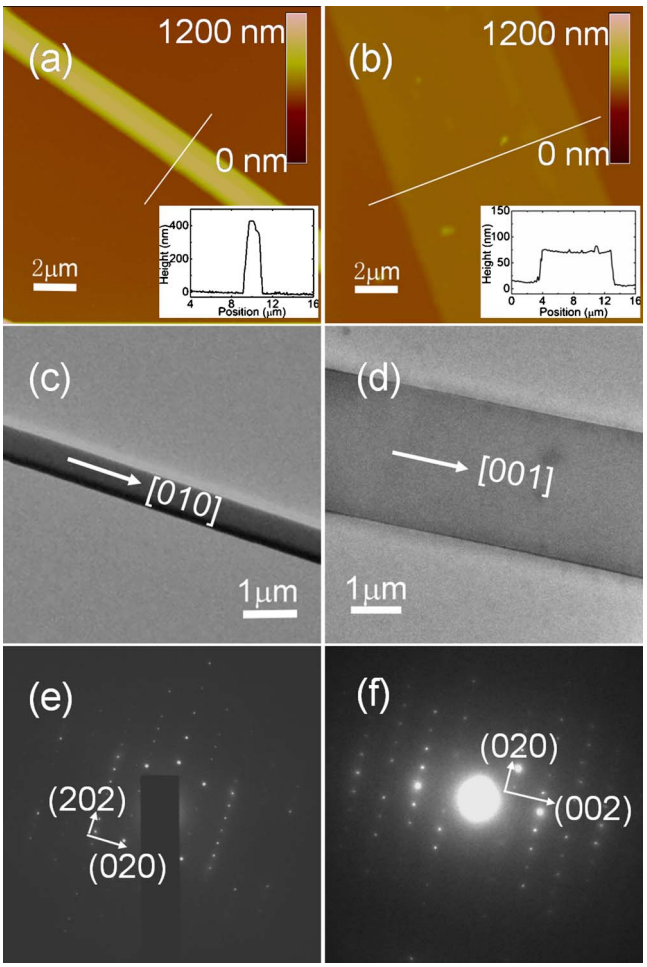

FIG. 2. (Color online) (a) and (b) AFM images (inset: Cross-section along the white line), (c) and (d) TEM images, and (e) and (f) SAED patterns of an individual rod and ribbon of BPEA. (a), (c), and (e): Rod; (b), (d), and (f): Ribbon.

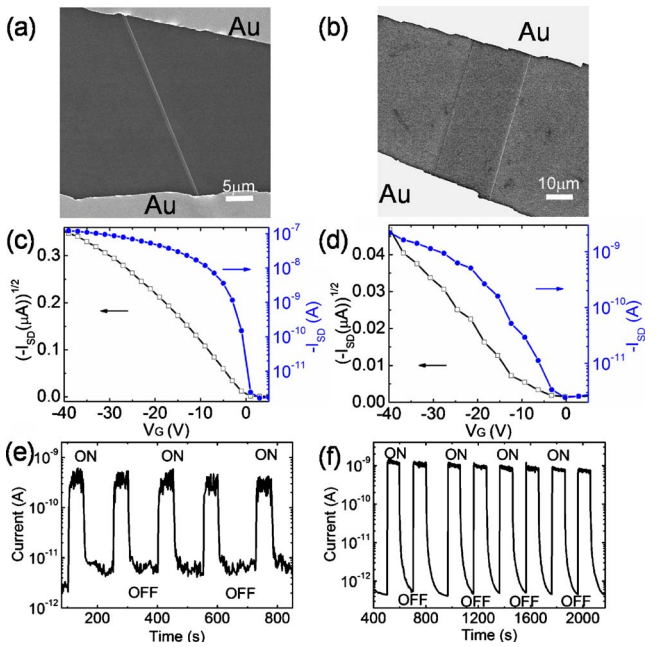

FIG. 3. (Color online) (a) and (b) The SEM images of an example device based on an individual single crystal micro/nanorod and ribbon of BPEA, (c) and (d) their corresponding field-effect transistor transfer curves, and (e) and (f) photoswitching characteristics of an individual micro/nanorod and ribbon devices (white light, light density 5.76 mw/cm^2, V=60 V). (a), (c), (e): Rod; (b), (d), (f): Ribbon.

solution of **BPEA** on n-octadecyltrichlorosilane (OTS) modified SiO_2 substrate, α phase micro/nanometer single crystals (rods) with a diameter about hundreds nanometers (usually between 500 nm and 1 μm) and length about hundreds micrometers were obtained.[15] When the solvent was changed to dichloromethane, micro/nanometer ribbons (width about several to tens micrometers and length about hundreds micrometers) were formed.[16] Figures 2(a) and 2(b) showed the atomic force microscopy (AFM) images of a typical micro/nanorod (thickness about 440 nm with width about 1.9 μm) and ribbon (thickness about 60 nm with width about 10 μm), we could see the ribbons were very thin, much thinner than the micro/nanorods. The different assembly morphologies indicated rods and ribbons might have different molecular packing. The transmission electron microscopy (TEM) images and their corresponding selected area electron diffraction (SAED) patterns of an individual micro/nanometer ribbon were shown in Figs. 2(d) and 2(f). No change in the SAED pattern was observed for the different parts of the same ribbon, indicating that the whole ribbon was a single crystal. From the SAED results, we could see the ribbons [Fig. 2(f)] have different structure and packing with rods [Fig. 2(e)],[15] and they belonged to β phase and grew along [001] (π-π stacking) direction. The morphologies and the prefer crystal growth direction of the ribbons were coincident very well with the theoretical calculated results by using Bravais–Friedel–Donnay–Harker (Ref. 17) model, which further proved the micro/nanoribbons casting from dichloromethane were β phase.

We are keen to know the charge transport properties of these β phase single crystals (ribbons), which would be helpful to understand the structure-property relationships and the charge transport mechanisms of organic semiconductors while comparing them to those of α phase. The devices were fabricated as follows: First, single crystal micro/nanoribbons of **BPEA** were grown directly on n-OTS modified SiO_2/Si substrates via drop-casting method from dichloromethane solution. Then the source-drain electrodes were constructed by manually gluing Au-films onto these micro/nanometer ribbons.[15,18] The channel was formed simultaneously, along with the lengths about twenty micrometers and the width depending on the ribbons themselves. Devices characteristics [Fig. 3(d)] showed the mobilities of β phase single crystals were less than 0.01 cm^2/V s, much lower than that of α phase single crystals (mobility up to 0.73 cm^2/V s).[15] Very interestingly, the ribbons exhibited high photoresponse with light/dark current ratio up to 6×10^3, one of the highest values for organic photoswitches (this light/dark current ratio was even rarely obtained in inorganic materials), while the light/dark current ratio of devices of α phase single crystals was much lower [$\sim10^2$, Figs. 3(e) and 3(f)].

These obvious optoelectronic property differences of the α and β phase single crystals should be attributed to (i) the different molecular conformations and arrangements of α and β phases; and (ii) the different working mechanisms of field-effect transistors and photoswitches. For the working mechanism of p-type OFETs, it can be briefly explained as follows:[19] When a negative gate voltage is applied, a large electric field at the organic/insulator interface is produced. This field induces charges in the semiconductor and shifts up

its highest occupied molecular orbital and lowest unoccupied molecular orbital (HOMO/LUMO) levels. When the gate voltage is large enough, the up-shifted HOMO level becomes resonant with the contact Fermi levels and electrons spill out of the semiconductor and into the contacts, and then positively charged holes are left. These holes are the mobile charges that moved in response to an applied drain voltage. In phase β, **BPEA** adopted nearly face-to-face packing and this packing would more facilitate carrier transport than that of phase α (typical herringbone packing). But **BPEA** displayed nonplanar conformation in phase β, and this nonplanar structure disrupted the conjugation of molecules (minimizing the π-conjugated system) and lowered the HOMO energy level of **BPEA**. The lower HOMO energy level would cause (i) larger mismatch between HOMO level of **BEPA** and Fermi level of electrodes; and (ii) lower carrier concentration at a given bias voltage. And these two factors should be responsible for the low mobility of β phase single crystals. As for photoswitches,[5,6,20,21] semiconductors absorbed light to form excitons first, and then the carriers (free holes and electrons) are generated by excitons dissociation. The generation of carriers also shifts the HOMO/LUMO levels of semiconductors to resonate with the Fermi levels of the electrodes as that of FETs. And then the current is observed when a bias voltage is applied. Since in photoswitches the carriers are generated by light, the lower HOMO energy levels of β phase crystals would not be the main factor to affect the device performance, and the nearly face-to-face packing in β phase more facilitate transporting the generated carriers than that of α phase single crystals. As a result, the β phase single crystals exhibit high photoswitch performance.

In conclusion, the control synthesis of α and β phase micro/nanosize single crystals of **BPEA** was achieved. The structures of these two phases were confirmed by AFM, SAED, micro-Raman spectra, and theoretical simulation. Devices of β phase single crystals exhibited very high photoswitch performance (on/off current ratio reached 6×10^3, one of the highest values reported for organic materials), and those of α phase displayed high field-effect performance. These quite distinct phenomena observed in two phases of **BPEA** would be helpful to understand the structure-property relationship and the different working mechanisms of field-effect transistors and photoswitches.

This work was supported by the National Natural Science Foundation of China (Grant Nos. 60736004 and 50873105), Ministry of Science and Technology of China (Grant Nos. 2006CB806200 and 2006CB932100), and Chinese Academy of Sciences (Ref. 22).

[1]E. Ahmed, A. L. Briseno, Y. Xia, and S. A. Jenekhe, J. Am. Chem. Soc. **130**, 1118 (2008).
[2]D. H. Kim, D. Y. Lee, H. S. Lee, W. H. Lee, Y. H. Kim, J. I. Han, and K. Cho, Adv. Mater. **19**, 678 (2007).
[3]K. Walzer, B. Maenning, M. Pfeiffer, and K. Leo, Chem. Rev. **107**, 1233 (2007).
[4]V. Coropceanu, J. Cornil, D. A. da Silva Filho, Y. Olivier, R. Silbey, and J.-L. Brédas, Chem. Rev. **107**, 926 (2007).
[5]Q. Tang, L. Li, Y. Song, Y. Liu, H. Li, W. Xu, Y. Liu, W. Hu, and D. Zhu, Adv. Mater. **19**, 2624 (2007).
[6]W. Zhao, Q. Tang, H. S. Chan, J. Xu, K. Y. Lo, and Q. Miao, Chem. Commun. (Cambridge) **2008**, 4324.
[7]H. Wu, Y. Sun, D. Lin, R. Zhang, C. Zhang, and W. Pan, Adv. Mater. **21**, 227 (2009).
[8]C. Yang, C. J. Barrelet, F. Capasso, and C. M. Lieber, Nano Lett. **6**, 2929 (2006).
[9]L. Jiang, Y. Fu, H. Li, and W. Hu, J. Am. Chem. Soc. **130**, 3937 (2008).
[10]Y. Zhou, L. Wang, J. Pei, and Y. Cao, Adv. Mater. **20**, 3745 (2008).
[11]Y. Zhang, P. Chen, L. Jiang, W. Hu, and M. Liu, J. Am. Chem. Soc. **131**, 2756 (2009).
[12]A. Zhu, J. O. White, and H. G. Drickamer, J. Phys. Chem. A **106**, 9209 (2002).
[13]Y. Zhao, J. Xu, A. Peng, H. Fu, Y. Ma, L. Jiang, and J. Yao, Angew. Chem., Int. Ed. **47**, 7301 (2008).
[14]R. Giménez, M. Piñol, and J. L. Serrano, Chem. Mater. **16**, 1377 (2004).
[15]C. Wang, Y. Liu, Z. Ji, E. Wang, R. Li, H. Jiang, Q. Tang, H. Li, and W. Hu, Chem. Mater. **21**, 2840 (2009).
[16]Small amounts of rods were also formed, micro-Raman spectrum and SEAD results showed these rods belonged to α phase.
[17]A. L. Briseno, S. C. B. Mannsfeld, X. Lu, Y. Xiong, S. A. Jenekhe, Z. Bao, and Y. Xia, Nano Lett. **7**, 668 (2007).
[18]Q. Tang, Y. Tong, Z. Ji, H. Li, W. Hu, Y. Liu, and D. Zhu, Adv. Mater. **20**, 1511 (2008).
[19]C. R. Newman, C. D. Frisbie, D. A. Da Silva Filho, J.-L. Brédas, P. C. Ewbank, and K. R. Mann, Chem. Mater. **16**, 4436 (2004).
[20]A. D. Schwab, D. E. Smith, B. Bond-Watts, D. E. Johnston, J. Hone, A. T. Johnson, J. C. de Paula, and W. F. Smith, Nano Lett. **4**, 1261 (2004).
[21]K. Oyaizu and H. Nishide, Adv. Mater. **21**, 2339 (2009).
[22]See supplementary material at http://dx.doi.org/10.1063/1.3383222 for details of the experimental section, SEM images, powder X-ray diffraction, micro-Raman spectra, field-effect, and photoswitches characteristics.